Shahrood University of Technology

Journal of Mining and Environment (JME)

Journal homepage: www.jme.shahroodut.ac.ir

Iranian Society of Mining Engineering (IRSME)

Exploring the Fracture Mechanics of Rock Salt through Punch Shear Testing: An Integrated Experimental and Computational Study

Amir Rezaei[1], Vahab Sarfarazi[2*], Mohammad Fatehi Marji[1], and Mohammad Omidimanesh[2]

1. Mining Engineering Department, Faculty of Mining, Metallurgical and Petroleum Engineering, Yazd University, Yazd, Iran
2. Mining Engineering Department, Hamedan University of Technology, Hamedan, Iran

Article Info

Received 23 September 2025
Received in Revised form 12 December 2025
Accepted 8 February 2026
Published online 8 February 2026

DOI: 10.22044/jme.2026.16878.3308

Keywords

Punch cutting test
Rock salt
Numerical modelling
PFC2D
Experimental test

Abstract

This study provides an in-depth examination of the failure characteristics of rock salt samples subjected to punch shear testing, emphasizing the analysis of fracture processes and the material's mechanical response. Given the diverse industrial applications of rock salt, the need for more detailed studies in this field is evident. The study employs an integrated approach combining practical experiments and numerical simulations using PFC2D software. The results reveal that the failure response of rock salt is governed by critical factors such as the loading rate and the material's inherent mechanical properties. Laboratory observations indicate that fractures primarily initiate from structurally weak zones, with stress concentration at contact areas being the main cause of tensile-shear failures in the samples. The findings of this study can serve as a foundation for establishing novel quality evaluation criteria for rock salt, underscoring the need for continued research efforts to improve safety and performance in related engineering applications.

1. Introduction

Investigating the failure characteristics of rock salt through punch shear testing is a crucial subject within materials science and geoscience disciplines, emphasizing a detailed examination of failure processes and the mechanical attributes of this material. Due to its extensive utilization across multiple sectors such as mining, civil infrastructure, and chemical containment, rock salt warrants thorough exploration. Punch shear testing is recognized as a standard technique for assessing material strength and failure responses, enabling the evaluation of rock salt's behavior under various loading scenarios in a controlled environment [1-4].

Recent studies have revealed that the failure response of rock salt is influenced by several factors, including the rate of loading, ambient temperature, and moisture levels. For example, research has demonstrated that an increase in loading rate can enhance the failure strength of rock salt [2]. Moreover, investigations into temperature effects indicate that elevated temperatures tend to cause rock salt to fail in a more ductile manner [5]. These insights improve our understanding of rock salt's performance under practical conditions and facilitate more reliable predictions regarding its behavior in engineering applications [6-8].

The integration of computational and experimental approaches provides more accurate insights. Numerical modeling can forecast failure patterns under diverse conditions, while laboratory experiments serve to verify these predictions [9]. For instance, a combined approach showed that numerical simulations accurately anticipated the failure behavior of rock salt under varying circumstances, with experimental data supporting these findings [10]. This synergy enhances our

Corresponding author: Sarfarazi@hut.ac.ir (V. Sarfarazi)

understanding of failure mechanisms and aids in the development of refined predictive models for rock salt behavior [11-15].

Additionally, advanced analytical methods such as X-ray tomography and electron microscopy contribute to a deeper understanding of the internal microstructure and failure processes [16]. These technologies allow for the visualization of microscopic structural changes during testing, offering a more comprehensive analysis of failure phenomena [17-20]. For example, microscopic observations have revealed that failure in rock salt often originates at zones of inherent structural weakness [21-23].

Ultimately, these research efforts can inform the establishment of improved testing protocols and evaluation standards for rock salt, promoting greater safety and efficiency in engineering projects involving this material [24]. Given the significance of this field, ongoing research and the acquisition of new experimental and computational data are essential to achieve a more holistic understanding of rock salt failure behaviour [25-29]. Future studies might focus on exploring the combined influence of multiple parameters on failure characteristics and developing sophisticated numerical models capable of simulating rock salt behaviour under more realistic conditions [30-33]. Recent studies have revealed that the failure response of rock salt is affected by several factors, including the rate of loading, ambient temperature, and moisture levels under uniaxial loading. In the present research, the failure behaviour of rock salt was investigated under punch testing. In this study, crack propagation at the microscale was simulated using Particle Flow Code (PFC).

3. Sampling

The subterranean salt mines of Garmsar, located in Semnan Province, Iran, are recognized as among the largest and most ancient salt reserves in the Middle East. These mines hold significant economic and industrial value due to the presence of salt domes featuring distinctive geomorphological formations and the high quality of the rock salt. Extraction of rock salt from these deposits is performed using several methods, including tunnel mining (see Figure 1a) and the room-and-pillar approach (see Figure 1b). These methods are widely employed because they reduce environmental impact and improve safety during operations. Additionally, the presence of diverse minerals in these mines makes them a valuable resource for various industries. From a geomechanical perspective, the Garmsar subterranean mines require detailed evaluations to predict the mechanical response of rock salt under different conditions. Due to its specific properties—including low elastic modulus and high cohesion—rock salt deforms readily under both dynamic and static loads. These properties are essential considerations in the design and development of tunnels and underground mines. Numerical modelling techniques, such as the finite element method, assist engineers in analysing tunnel stability and identifying potential weaknesses. Furthermore, predicting collapses and analysing loadings caused by the weight of overlying rocks and lateral pressures are among the primary challenges in extracting rock salt from these mines.

(a) (b)

Figure 1. Extraction methods in the underground mines of Garmsar: a) use of access tunnels; b) support using rock pillars.

The samples used for this study were obtained from the underground salt mines of Garmsar. These samples were collected using a laboratory core drilling machine with a standard diameter of 54 mm from the intact rock (Figure 2).

4. Experimental tests

After the samples were carefully extracted using the core drilling machine, it is important to note that all samples have lengths of 130 mm, 160 mm, and 240 mm, with a diameter of 54 mm (Table 1). These length values were selected according to the ISRM suggested method. These samples are then subjected to a punch shear test (Figure 3).

For this test, the samples are positioned vertically on two identical plates (Figure 4a) that flank the model from the left and right sides. Furthermore, an additional plate is positioned atop the model to ensure that the testing conditions are fully satisfied.

Figure 2. Standard core sampling from an intact salt block.

(a) (b) (c)

Figure 3. Cores used in the punch cutting test: a) 240 mm, b) 160 mm, c) 130 mm

(a) (b) (c)

Figure 4. a) Arrangement of the sample on the two lower plates; b) Placement of the third plate on the sample; c) Arrangement of the sample in the uniaxial testing machine.

This procedure is clearly demonstrated in Figure 4b. After preparation, the models are positioned within the uniaxial testing machine in a consistent manner, as shown in Figure 4c. These steps are performed to guarantee the precision and reliability of the test, enabling us to acquire dependable data from the punch shear experiment. By employing this approach, a more accurate evaluation of the mechanical behavior of the samples under various conditions can be achieved.

Once the sample is fully installed in the testing apparatus, the grips of the uniaxial testing machine begin the loading process with meticulous control. The loading speed is carefully set at 0.005 mm/s, and this slow, continuous force is applied to the upper plate, which is in direct contact with the sample's top surface. This is within the range of static loading conditions according to the ISRM suggested method.

This gradual loading is precisely regulated to ensure that the stress is evenly distributed throughout the sample as it experiences punch shear conditions (see Figure 5).

This controlled loading method is absolutely critical for preventing data contamination and avoiding unintended damage to the sample's structure. The device's precise mechanism enables measurement of the sample's deformation and resistance to applied loads with the highest possible accuracy. To ensure test validity, all parameters including loading speed, deformation amount, and sample resistance are recorded and monitored in real-time. This level of experimental precision allows researchers to thoroughly examine the material's mechanical behavior under realistically simulated conditions and obtain reliable data for subsequent analysis.

To gain a better understanding of the tensile and compressive resistance of the samples, they were subjected to Brazilian and uniaxial tests (Figure 6). These tests allow us to examine the mechanical behavior of the samples under various loading conditions. The Brazilian test is specifically designed to measure the tensile strength of materials under indirect conditions, while the uniaxial test provides precise information about the compressive resistance of the samples. The findings from these experiments are summarized in Table 1 and provide valuable insights into the mechanical characteristics of the materials and their behavior under various loading conditions [28, 29].

Figure 5. Punch cutting test

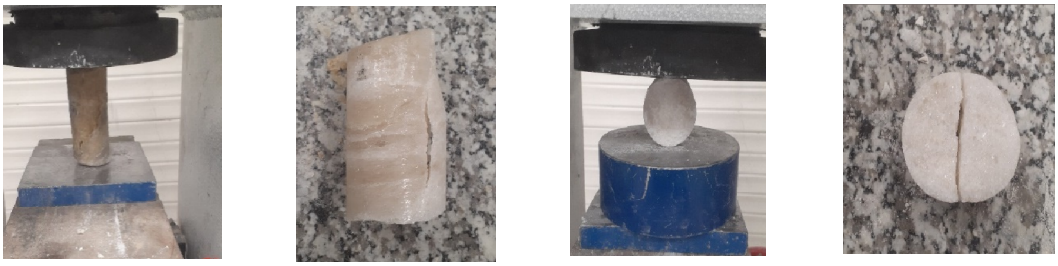

(a) **(b)** **(c)** **(d)**

Figure 6. Compressive strength test and Brazilian test

5. Failure pattern

Figure 7 clearly illustrates the failure pattern of laboratory cores and provides important details regarding the behavior of these cores under loading conditions. As can be observed, shear cracks initiate from the edges of the upper plate that is positioned on the model. These cracks gradually and steadily propagate downward towards the lower edge of the plate. This process demonstrates a specific pattern in the failure of the cores, which can aid us in gaining a better understanding of the failure mechanisms involved.

In fact, these shear cracks act as indicators of the internal stresses that arise due to loading. As these cracks progress, significant changes in the structure of the core will occur, which can ultimately lead to its final failure. Ultimately, these shear cracks result in a punch shear failure in the sample.

(a) (b) (c)

Figure 7. Failure pattern of models a) 240 mm, b) 160 mm, c) 130 mm

The cause of crack formation in the model is due to the concentration of shear force at the point of contact between the upper plate and the sample. This force concentration generates high stresses in the contact area, which can lead to the formation of cracks. In fact, when a force is applied to a specific area of the material, the distribution of stresses does not occur uniformly, resulting in certain regions being subjected to greater pressure. This additional pressure can initiate primary cracks that gradually propagate with continued loading.

Furthermore, the presence of internal cracks in the structure of rock salt also acts as weak points and can accelerate the punch shear process. These cracks serve as stress concentration points, thereby increasing the likelihood of failure in these areas.

6. Numerical models

6.1. PFC model

PFC, known as Particle Flow Code, is advanced and specialized software designed specifically for geotechnical simulations. This software enables engineers and researchers to model the behavior of various materials commonly encountered in mining engineering and soil mechanics projects. In these fields, a precise understanding of how materials react under different stresses and conditions is of paramount importance, and PFC serves as an efficient tool in this regard.

One notable feature of this software is its ability to analyze the behavior of discontinuous materials, which is particularly relevant for many geological and granular substances. PFC employs the discrete element method (DEM) for simulating this behavior, a numerical technique that facilitates the simulation of interactions between individual particles or elements. This method allows us to obtain a detailed and realistic representation of material responses in scenarios involving fracturing, yielding, and large deformations.

Furthermore, PFC is highly versatile in its applications, as it can perform simulations in both two-dimensional and three-dimensional environments. This capability allows engineers and researchers to select the most appropriate level of detail based on their specific modeling needs and computational resources. Overall, PFC is a valuable tool for analyzing and understanding material behavior under various conditions, contributing to the improvement of design and execution processes in engineering projects.

The term fat-jointed material (FJM) describes the assembly of particles connected by FJs. The boundary separating the faceted grains lies within elements that may be either bonded or unbonded. In this framework, the FJ is located at the interface between grains. Furthermore, the forces and moments, initially set to zero, are updated based on the force-displacement relationship governing the relative motion between the bond and the surface. Both direct and incremental methods are used to update the normal and shear forces. The bonded element exhibits linear elastic behavior until its strength surpasses a predefined threshold. This model allows us to simulate the behavior of particles under various conditions and provides a better understanding of the interactions between grains and their effects on the overall properties of materials. Maximum normal and shear stresses of element ($\sigma max(e)$, $\tau max(e)$) are calculated by subsequent formulas:

$$\sigma_{max}^{(e)} = \frac{-F_{(e)}^{-n}}{A^{(e)}}$$

$$\tau_{max}^{(e)} = \frac{F_{(e)}^{-s}}{A^{(e)}}$$

$A^{(e)}$ is element area, while $-F_{(e)}^{-n}$ and $-F_{(e)}^{-s}$ denote the normal and shear forces, respectively, acting on the component [30–34].

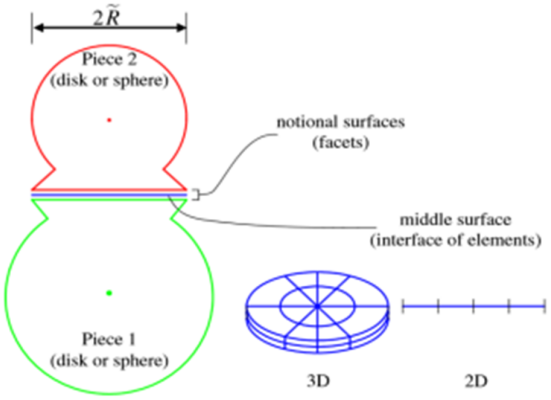

Figure 8. Flat-joint model [33]

6.2. PFC2D model preparation and calibration for salt rock

PFC2D assembly test models were constructed following the standard procedure detailed [32], including particle generation, packing, isotropic stress initialization, floater removal, and bond installation. Given the small sample size, the influence of gravity and its associated stress gradient on macroscopic behavior was negligible. A validated PFC particle assembly was generated using micro-characteristics (Table 1).

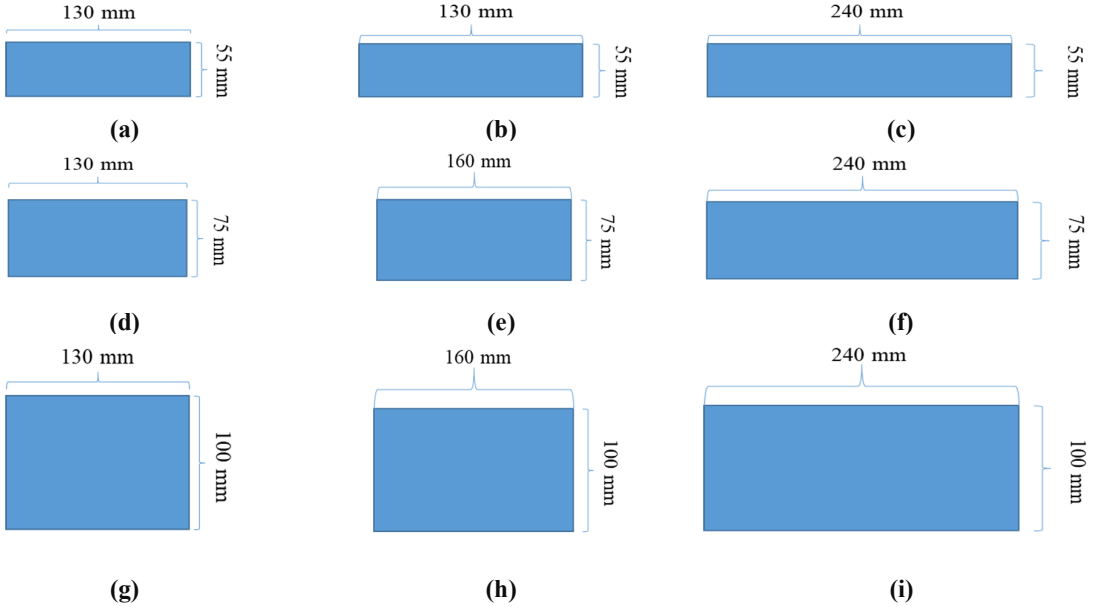

Figure 9. Schematic of the Numerical Modeling

Figure 10 illustrates the models created in the PFC2D software. The dimensions constructed in the software space are divided into three sections:

1. Diameter (width) of 55 mm and lengths of 130 mm, 160 mm, and 240 mm (Fig. 10 a-c).
2. Diameter (width) of 75 mm and lengths of 130 mm and 240 mm (Fig. 10 d-f).
3. Diameter (width) of 100 mm and lengths of 130 mm and 240 mm (Fig. 10 g-i).

Figure 9 shows a schematic of the numerical modelling and their dimensions. These parameters have been chosen for Testing of the cores.

Macro mechanical properties of rock such as Brazilian tensile strength was calibrated by adjusting the micro parameters reported in Table 1. By changing the micro parameters in a try and error manner, macro mechanical properties will be calibrated.

Table 1. Proper micro-properties

Particle micro properties		Flat-joint micro properties	
diameter (mm)	55,75 100	Gap ratio	0.5
height (mm)	130,160240	Elasticity modulus (GPa)	20
Normal to shear stiffness ratio (Kn/ks)	1.9	Friction angle (°)	0.5
Density (kg/m^3)	2900	Tensile strength (MPa)	21
particle diameter (minimum) (mm)	0.5	Tensile strength (standard deviation) (MPa)	2.1
particle diameter (maximum) (mm)	1.1	Cohesion (MPa)	30
Elasticity modulus (GPa)	20	Cohesion (standard deviation) (MPa)	3
Ratio of standard stiffness to shear stiffness (Kn/ks)	1.9	Elements	2

6.3. Failure pattern

Figure 11 depicts the fracture patterns observed in the samples subjected to punch testing. In all models, the fracture pattern clearly demonstrates shear failure. Specifically, tensile and shear cracks originate at the interface between the segment and the salt sample, propagating parallel to the loading

axis and eventually linking with opposing cracks. Notably, the quantity of shear cracks exceeds that of tensile cracks.

Examining Figure 12, which depicts the chain of contact forces prior to load application, it becomes evident that tensile stress is highly concentrated at the interfaces between the plates and the model. This localized tensile stress is identified as the primary cause of tensile crack initiation. In the illustration, black lines indicate areas of compressive stress concentration, while red lines highlight regions under tensile stress. The use of these distinct colors effectively illustrates how different stress types at contact points influence crack development. This evaluation provides valuable insights into failure processes and crack propagation within numerical simulations.

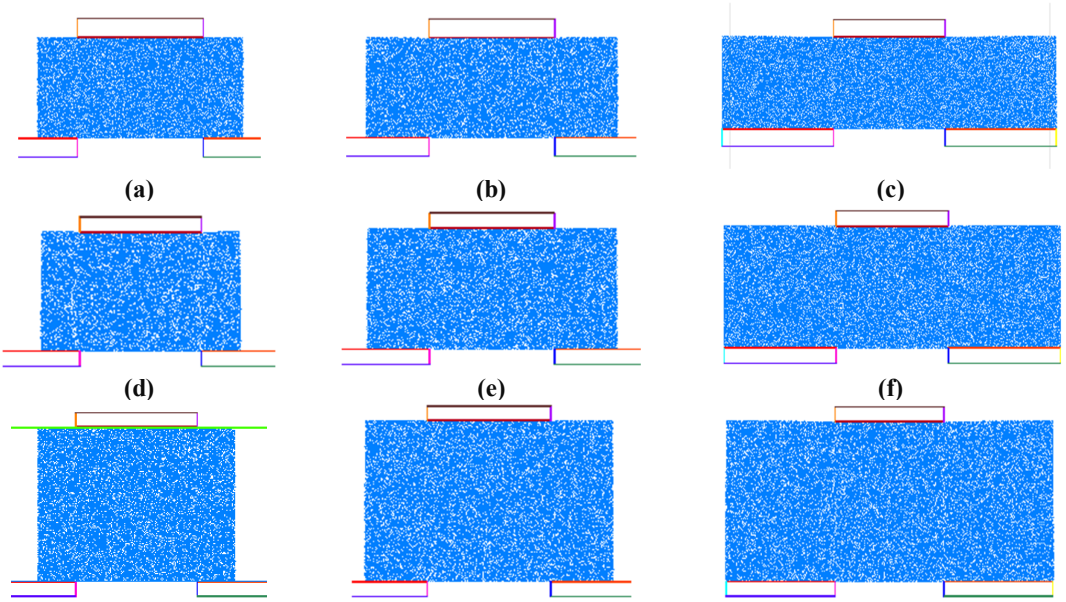

Figure 10. Numerical Models

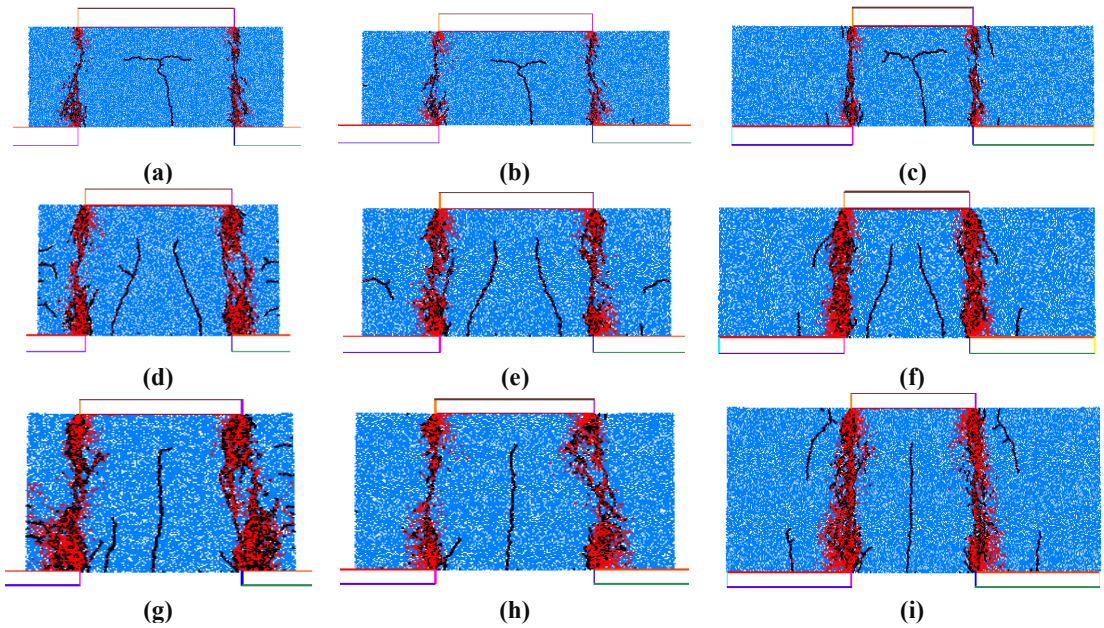

Figure 11. Failure pattern numerical model

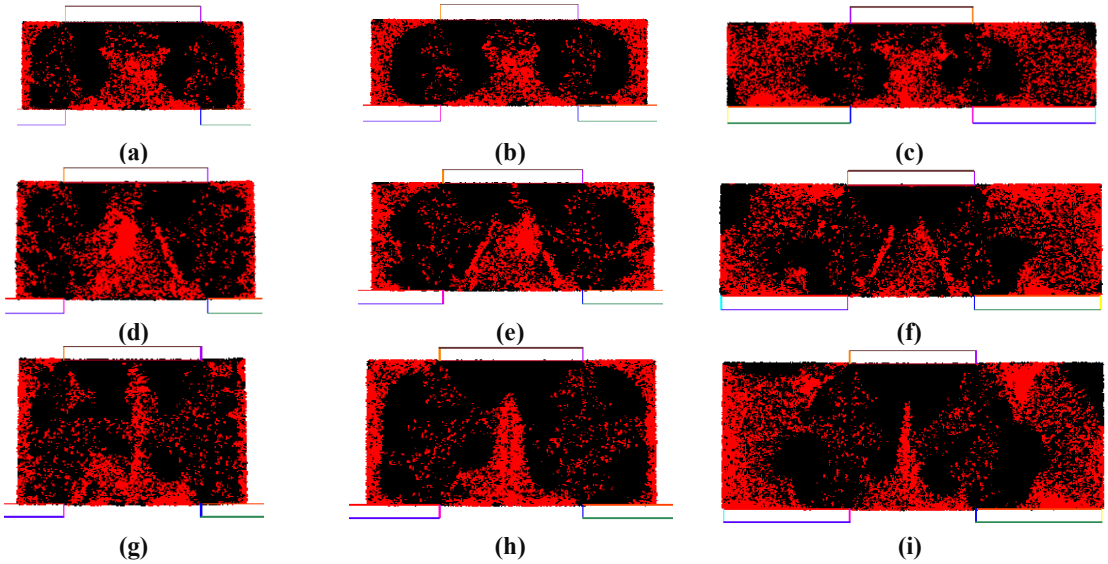

Figure 12. Contact force chain numerical model

6.4. Rose diagram

Figure 13 presents the crack propagation patterns observed in the punch test models. Most cracks form at angles of 0 degrees and 180 degrees relative to the loading direction. This trend becomes more evident as the thickness of the sample decreases. Conversely, when the sample thickness increases, cracks oriented at approximately 20 degrees and 160 degrees start to appear. Essentially, thinner samples bring the top and bottom surfaces closer, intensifying stress interactions between these surfaces and resulting in cracks aligned at 0 and 180 degrees. In contrast, thicker samples reduce this surface interaction, allowing cracks to develop in a wider range of orientations within the material.

6.5. The effect of sample height and sample length on shear strength and shear stiffness

Figure 14 shows how the height of the sample affects the shear strength of rock salt, presenting both numerical simulations and experimental findings. As the sample height increases, the shear strength decreases, which is explained by the growth of defects such as dislocations and weak intergranular bonds along the shear plane. The numerical data closely matches the experimental observations.

In Figure 15, the relationship between sample length and the shear strength of rock salt is illustrated, with results given for different sample heights. For a fixed sample height, the shear strength declines as the sample length becomes longer.

Figure 16 highlights the effect of sample height on the shear stiffness of rock salt, including both numerical and experimental results. An increase in sample height leads to a reduction in shear stiffness, attributed to the increased presence of weaknesses along the shear path. The numerical outcomes show good agreement with the experimental measurements.

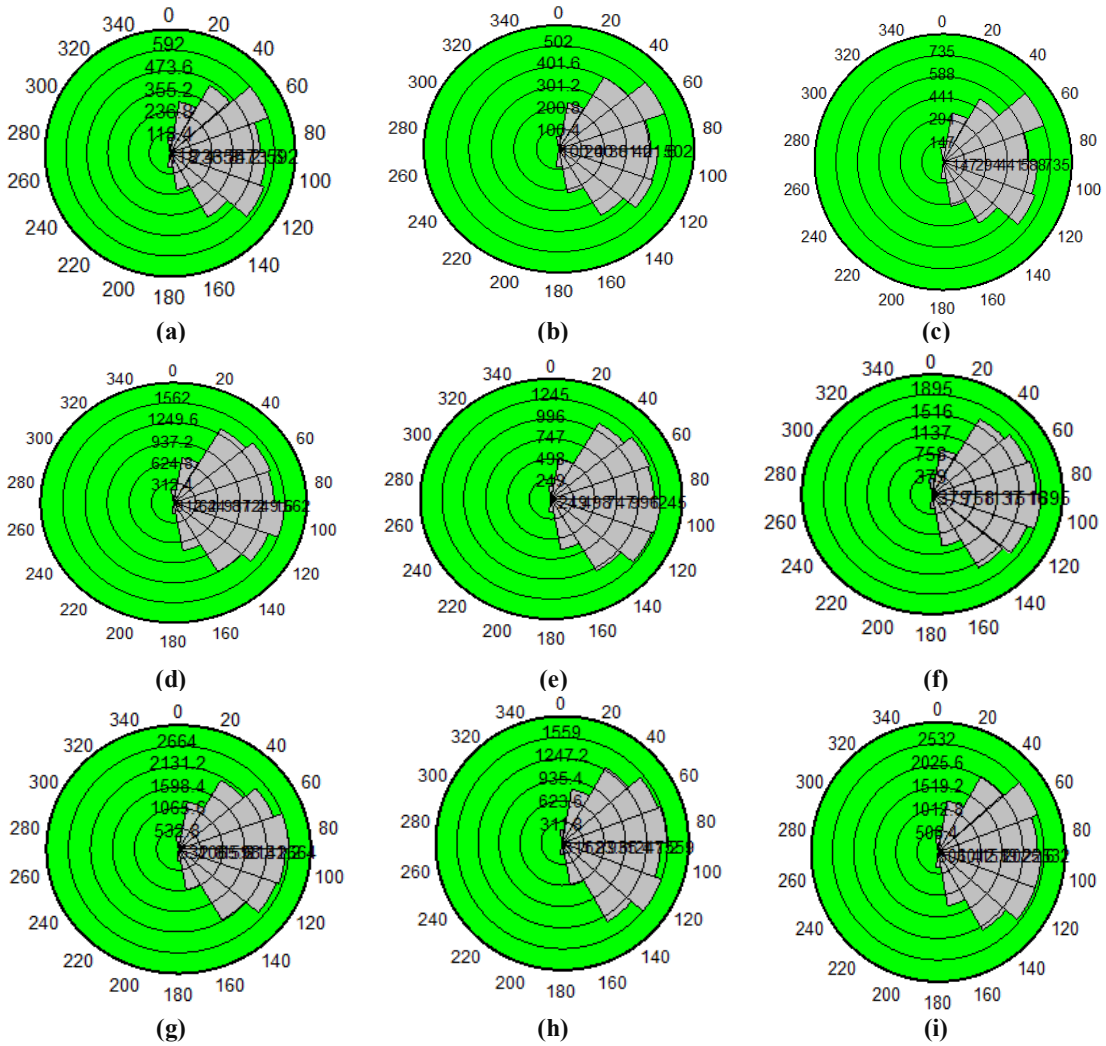

Figure 13. Rose diagrams of numerical models

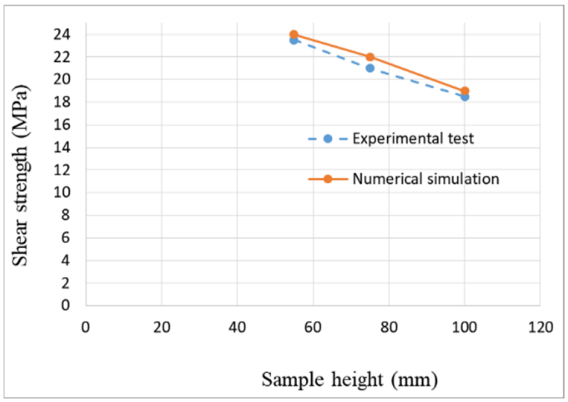

Figure 14. The effect of sample height on shear strength

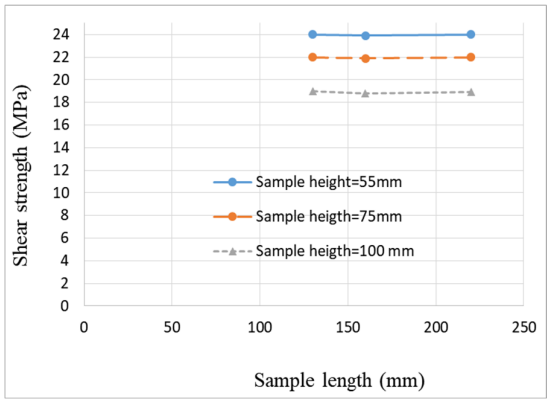

Figure 15. The effect of sample length on shear strength

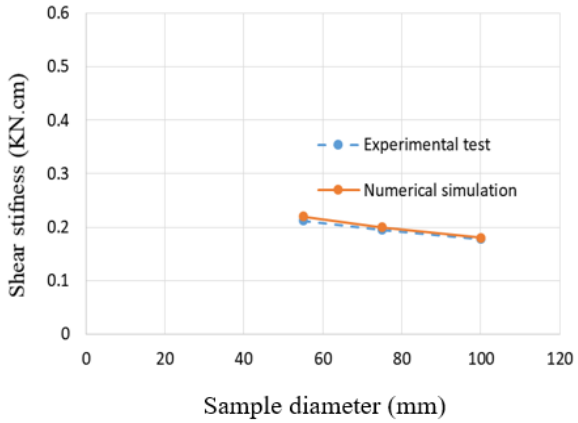

Figure 16. Effect of specimen height on shear stiffness: numerical and experimental results.

Figures 17a-c present the stress-strain relationship plotted against cumulative fracture count for models with diameters of 55 mm, 75 mm, and 100 mm. These illustrations reveal three distinct behavioral phases: the elastic deformation regime, the plastic deformation region, and the ultimate rupture point.

Prior to reaching the elastic threshold in the simulation, the specimens exhibit no measurable cracking activity. As loading intensifies, fracture initiation events begin accumulating.

During elastic deformation, the models demonstrate consistent linear elastic behavior accompanied by a steady increase in microfracture occurrences. Transitioning beyond this phase, the stress-strain response becomes nonlinear, with progressively accelerating fracture propagation until reaching maximum load capacity, at which point crack coalescence dominates.

Noteworthy fluctuations occur before peak stress conditions, attributable to interactions between primary fracture networks. Following this apex, microfracture frequency diminishes relative to expanding crack populations. The specimens exhibit abrupt stress deterioration upon reaching their load-bearing limits, with pronounced post-peak stress declines indicating comprehensive macroscale failure throughout the modeled structures.

Empirical observations suggest an inverse correlation between the magnitude of stress reduction and microfracture density, supporting the theoretical premise that sustained loading conditions generate discrete stress drops, each corresponding to fracture cluster formation events.

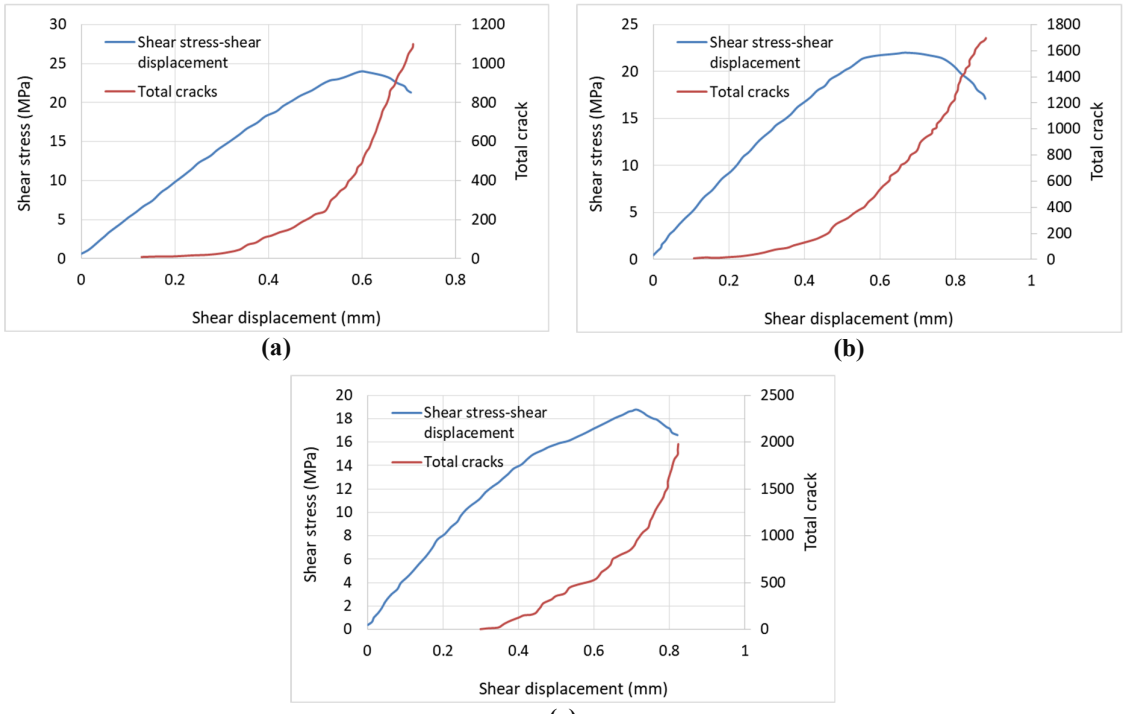

Figure 17. Stress-strain curve along the total crack number for model height of a) 55 mm, b) 75mm, and c) 100 mm.

7. Discussion

Rock salt, as a creeping rock, has a significant impact on the stability of underground spaces. Studying the shear behavior of rock salt can provide an ideal understanding of failure modes and reveal its shear strength. To investigate the effect of scale on the fracture behavior of rock salt, samples of different dimensions were prepared and subjected to punch shear tests.

The shear strength of rock salt is a function of its fracture pattern. In general, three types of fracture were observed. The first type of fracture is the fracture along the cleavage planes in the salt sample. In this case, the fracture strength of the salt sample and its hardness are minimal. Even the displacement corresponding to the fracture stress is minimum. That is, by applying a small displacement to the surfaces of the flaking, the stress is quickly distributed across the flaking surface and causes failure along these surfaces. The low shear strength in this condition also stems from the same issue. The second type of failure is flexural failure in the center of the salt sample. In this condition, the resistance of the rock salt is slightly higher than in the previous case. In this condition, the tensile stress in the center of the sample reaches a critical level, causing tensile failure in the central part. In this case, the crack growth is unstable. In other words, when a tensile crack is created, without applying more stress, the crack grows in a splitting manner and causes the sample to fail. The third type of failure is shear failure at the point of load application. In this condition, the strength of the sample is higher than in the previous cases and the crack growth is stable. That is, with the formation of shear cracks, its growth stops. When the stress level increases, the shear crack grows again. Accordingly, the shear stiffness of the salt sample and the shear displacement corresponding to the fracture stress are higher than the values obtained in other fractures.

8. Conclusions

This research utilizes a combined methodology, incorporating both laboratory experiments and numerical modeling with PFC2D software, to explore the shear response of rock salt during punch testing. The results reveal that:

- The failure behavior of rock salt is influenced by key parameters, including the loading rate and the material's intrinsic mechanical properties.
- Fractures primarily initiate from structurally weak zones, with stress concentration at contact areas being the main cause of tensile-shear failures in the samples.
- The shear strength was decreased by increasing the model scale.
- Shear stiffness was decreased by increasing the model scale.
- Experimental results were in a good accordance with numerical outputs.

Conflict of interest

The authors have no financial relationships with governmental agencies or organizational affiliations that could have an inappropriate influence on the work.

References

[1]. Hosseini, M., & Khodayari, A. R. (2018). Effects of temperature and confining pressure on mode II fracture toughness of rocks (Case study: Lushan Sandstone). *Journal of Mining and Environment, 9*(2), 379-391.

[2]. Jabari, A., & Hosseini, M. (2017). An overview of the most common tests of the mode II fracture toughness performed on rock specimens. 10th National Congress on Civil Engineering. Faculty of Civil Engineering. Sharif University of Technology.

[3]. Huang. S., Lu, J., Wang, J., Fu, X., Fu, Y., Li, Y., Shi, X., Dong, Z., Zhao, K., Li, P., Xu, M., & Chen, X. (2024). Experimental study on creep characteristics of electrolyte-bearing salt rock under long-term triaxial cyclic loading. *Front. Earth Sci. 12:*1503158.

[4]. Kolano, M., Cała, M., & Stopkowicz, A. (2024). Mechanical Properties of Rock Salt from the Kłodawa Salt Dome A Statistical Analysis of Geomechanical Data. *Materials*, *17*(14), 3564.

[5]. Schulze, O. (2017). Investigations on damage and healing of rock salt. In The Mechanical Behavior of Salt–Understanding of THMC Processes in Salt (pp. 33-43). CRC Press.

[6]. Han, Y., Ma, H., Yang, C., Li, H., & Yang, J. (2021). The mechanical behavior of rock salt under different confining pressure unloading rates during compressed air energy storage (CAES). *Journal of Petroleum Science and Engineering*, *196*, 107676.

[7]. Liang, W. G., Zhao, Y. S., Xu, S. G., & Dusseault, M. B. (2011). Effect of strain rate on the mechanical properties of salt rock. *International Journal of Rock Mechanics and Mining Sciences*, *48*(1), 161-167.

[8]. Wisetsaen, S., Walsri, C., & Fuenkajorn, K. (2015). Effects of loading rate and temperature on tensile strength and deformation of rock salt. *International Journal of Rock Mechanics and Mining Sciences, 73,* 10-14.

[9]. Qian, W., Wu, S., Lei, L., Hu, Q., & Liu, C. (2024). Time lapse in situ X-ray imaging of failure in structural materials under cyclic loads and extreme environments. *Journal of Materials Science & Technology, 175,* 80-103.

[10]. Zheng, Z., Wang, G., Hu, X., Niu, C., Ma, H., Liao, Y., & Yang, C. (2024). Microstructural evolution and mechanical behaviors of rock salt in energy storage: A molecular dynamics approach. *International Journal of Rock Mechanics and Mining Sciences, 182,* 105882.

[11]. Shad, S., Razaghi, N., Zivar, D., & Mellat, S. (2023). Mechanical behavior of salt rocks: A geomechanical model. *Petroleum, 9*(4), 508-525.

[12]. Liang, K., Xie, L., He, B., Zhao, P., Zhang, Y., & Hu, W. (2021). Effects of grain size distributions on the macro-mechanical behavior of rock salt using micro-based multiscale methods. *International Journal of Rock Mechanics and Mining Sciences, 138,* 104592.

[13]. Chang, J., Qi, Y., Yang, R., & Hao, T. (2025). The self-healing property of rock salt damage in underground gas storage: A review. *Results in Engineering*, 106098.

[14]. Li, D., Liu, W., Li, X., Tang, H., Xu, G., Jiang, D., & Fan, J. (2022). Physical simulation and feasibility evaluation for construction of salt cavern energy storage with recycled light brine under gas blanket. *Journal of Energy Storage, 55,* 105643.

[15]. Fourmeau, M., Liu, W., Li, Z., Nelias, D., Fan, J., Tian, H., & Liu, W. (2025). Research status of creep–fatigue characteristics of salt rocks and stability of compressed air storage in salt caverns. *Earth Energy Science, 1*(1)*,* 98-116.

[16]. Liu, Y., & Dai, F. (2021). A review of experimental and theoretical research on the deformation and failure behavior of rocks subjected to cyclic loading. *Journal of Rock Mechanics and Geotechnical Engineering, 13*(5), 1203-1230.

[17]. Zubair, M., Ullah, S., & Emad, M. Z. (2025). Numerical and Experimental Investigation of the Creep Behavior of Rocksalt Pillars: A Case Study. *Rock Mechanics Letters, 2*(2), 125-131.

[18]. Wong, L. N. Y., & Zhao, K. (2025). Numerical analysis of triaxial creep-fatigue interaction of rock salt. *Journal of Rock Mechanics and Geotechnical Engineering, 12*(6):78-97.

[19]. Azabou, M., Rouabhi, A., & Blanco-Martìn, L. (2021). Effect of insoluble materials on the volumetric behavior of rock salt. *Journal of Rock Mechanics and Geotechnical Engineering, 13*(1), 84-97.

[20]. Reffas, S. A., Elmeguenni, M., Zagane, M. S., Moulgada, A., Yaylaci, M., Yekhlef, R., & Yaylaci, E. U. (2025). Experimental research of polymer fracture under hydro-mechanical behavior. *Geomechanics and Engineering, 41*(3), 337–349.

[21]. Baltach, A., Benhamena, A., Chaouch, M. I., Zagane, M. E.-S., Yaylaci, M., Ozturk, S., & Yaylaci, E. U. (2025). Numerical analysis of crack nucleation in contact mechanics under fretting wear loading. *Structural Engineering and Mechanics, 94*(3), 231–238.

[22]. Yaylaci, M. (2016). The investigation crack problem through numerical analysis. *Structural Engineering and Mechanics, 57*(6), 1143–1156.

[23]. Yaylaci, M., Yaylaci, E. U., Turan, M., Ozdemir, M. E., Ozturk, S., & Ay, S. (2024). Research of the crack problem of a functionally graded layer. *Steel and Composite Structures, 50*(1), 77–87.

[24]. Yaylaci, M. (2022). Simulate of edge and an internal crack problem and estimation of stress intensity factor through finite element method. *Advances in Nano Research, 12*(4), 405–414.

[25]. Yaylaci, M., YayIaci, E.U., Ozdemir, M.E., Ay, A., & Ozturk, S., (2022). Implementation of finite element and artificial neural network methods to analyze the contact problem of a functionally graded layer containing crack. *Steel and Composite Structures, 45*(4), 501–514.

[26]. Benouis, A., Zagane, M., Moulgada, A., Yaylaci M., Kaci, D., Terzi, M., Özdemir, M., & Yaylaci, E.U. (2024). Finite element analysis of the behavior of elliptical cracks emanating from the orthopedic cement interface in total hip prostheses. *Structural Engineering and Mechanics, 89*(5), 539–547.

[27]. Yaylacı, M., Yaylacı, E. U., Özdemir, M. E., Öztürk, Ş., & Sesli, H. (2023). Vibration and buckling analyses of FGM beam with edge crack: Finite element and multilayer perceptron methods. *Steel and Composite Structures, 46*(4), 565–575.

[28]. Bieniawski, Z,T & Haweks,I (1978). Suggested methods for determining tensile strength of rock materials. Suggested method for determining indirect tensile strength by Brazilian test. Commission on Standardization of Laboratory and Field Tests, *Int J Rock Mech Min Sci. 15*,102–103.

[29]. Bieniawski, Z,T & Haweks,I (1979). Suggested methods for determining the uniaxial compressive strength and deformability of rock materials. *Int J Rock Mech Min Sci, 16*(2),135–140.

[30]. Potyondy D.O., & Cundall PA. (2004) A bonded-particle model for rock. *Int J Rock Mech Min Sci 41*,1329–1364.

[31]. Potyondy, D.O. (2017). Simulating perforation damage with a flat-jointed bonded-particle material. Paper presented at the 51st US Rock Mechanics/Geomechanics Symposium, San Francisco, California, USA.

[32]. Potyondy, D.O. (2015). The bonded-particle model as a tool for rock mechanics research and application: current trends and future directions. *Geosyst Eng, 18*(1), 1–28.

[33]. Potyondy, D.O. (2012). A fat-jointed bonded-particle material for hard rock. Paper presented at the 46th U.S. Rock Mechanics/Geomechanics Symposium, Chicago, USA.

انجمن مهندسی معدن ایران
نشریه مهندسی معدن و محیط زیست
نشانی نشریه: www.jme.shahroodut.ac.ir
دانشگاه صنعتی شاهرود

بررسی مکانیک شکست سنگ نمک از طریق آزمایش برش پانچ: یک مطالعه تجربی و محاسباتی

امیر رضایی[1]، وهاب سرفرازی[2*]، محمد فاتحی مرجی[1] و محمد امیدی منش[1]

۱. بخش مهندسی معدن، دانشکده مهندسی معدن، متالورژی و نفت، دانشگاه یزد، یزد، ایران
۲. گروه مهندسی معدن، دانشگاه صنعتی همدان، همدان، ایران

اطلاعات مقاله

تاریخ ارسال: ۲۰۲۵/۰۹/۲۳
تاریخ داوری: ۲۰۲۵/۱۲/۱۲
تاریخ پذیرش: ۲۰۲۶/۰۲/۰۸

DOI: 10.22044/jme.2026.16878.3308

کلمات کلیدی

آزمایش برش پانچ
سنگ نمک
مدلسازی عددی
PFC2D
آزمون آزمایشگاهی

چکیده

این مطالعه، بررسی عمیقی از ویژگی‌های شکست نمونه‌های نمک سنگ تحت آزمایش برش پانچ ارائه می‌دهد و بر تحلیل فرآیندهای شکست و پاسخ مکانیکی ماده تأکید دارد. با توجه به کاربردهای متنوع صنعتی نمک سنگ، نیاز به مطالعات دقیق‌تر در این زمینه مشهود است. این مطالعه از یک رویکرد یکپارچه با ترکیب آزمایش‌های عملی و شبیه‌سازی‌های عددی با استفاده از نرم‌افزار PFC2D استفاده می‌کند. نتایج نشان می‌دهد که پاسخ شکست نمک سنگ توسط عوامل حیاتی مانند نرخ بارگذاری و خواص مکانیکی ذاتی ماده کنترل می‌شود. مشاهدات آزمایشگاهی نشان می‌دهد که شکستگی‌ها در درجه اول از مناطق ضعیف ساختاری شروع می‌شوند و تمرکز تنش در نواحی تماس، علت اصلی شکست‌های کششی-برشی در نمونه‌ها است. یافته‌های این مطالعه می‌تواند به عنوان پایه‌ای برای ایجاد معیارهای ارزیابی کیفیت جدید برای نمک سنگ عمل کند و بر نیاز به تلاش‌های تحقیقاتی مداوم برای بهبود ایمنی و عملکرد در کاربردهای مهندسی مرتبط تأکید کند.

نویسنده مسئول مکاتبات. *Sarfarazi@hut.ac.ir* **(و. سرفرازی)**